Exp. Theo. NANOTECHNOLOGY 3 (2019) 103–114 https://doi.org/10.56053/3.1.103

Analytical studies of electrohydrodynamically TiO_2 nanostructure

*W. Gibbs, M. Torris**

Materials Engineering, The University of Queensland, Queensland 4072, Australia
*) Email: Torm@uq.edu.au

Received 13/8/2018, *Accepted* 28/12/2018, *Accepted* 15/1/2019

In this paper, we report an alternate technique for the deposition of nanostructured TiO_2 thin films using the electrohydrodynamic atomization (EHDA) technique us- ing polyvinylpyrrolidone (PVP) as a stabilizer. The required parameters for achieving uniform TiO_2 films using EHDA are also discussed in detail. X-ray diffraction results con- firm that the TiO_2 films were oriented in the anatase phase. Scanning electron microscope studies revealed the uniform deposition of the TiO_2. The purity of the films is charac- terized by using Fourier transform infrared (FTIR) spec- troscopy and X-ray photoelectron spectroscopy (XPS), con- firming the presence of Ti–O bonding in the films without any organic residue. The optical properties of the TiO_2 films were measured by UV-visible spectroscopy, which shows that the transparency of the films is nearly 85% in the visi- ble region. The current–voltage (I–V) curve of the TiO_2 thin films shows a nearly linear behavior with 45 mQ cm of elec- trical resistivity. These results suggest that TiO_2 thin films deposited via the EHDA method possess promising applications in optoelectronic devices.

Keywords: TiO_2; Analysis; Optical.

1. INTRODUCTION

The unique and intriguing properties of nanostructured thin films have prompted tremendous motivation among re- searchers to explore the possibilities of using them in technological applications. In particular, the optical and electronic properties of nanostructured thin films have been of very high interest due to their potential applications in the fabrication of microelectronic and optoelectronic de- vices [1, 2]. The performance of the thin films for device applications is highly influenced by the crystallite size, morphology, phase and impurity type concentration [3]. There is always an increasing demand for new technology for the fabrication of nanostructured thin films for functional de- vices in order to control the phase purity, the morphology and the surface properties at the nanoscale, which is of great interest to deliver distinctive properties. In this regard, many studies have been recently carried out to produce surfaces and films by tailoring the nanostructure.

Exp. Theo. NANOTECHNOLOGY 3 (2019) 103-114

Nanostructured thin films of titanium dioxide (TiO_2) have been regarded as the subject of a great deal of research due to its exceptional chemical, electrical and optical properties and its potential applications in diverse fields such as (i) optoelectronics, (ii) photocatalysis, (iii) solar cells, rial activity etc. [4–6]. Generally, TiO_2 nanostructured films exist in two phases, viz. (a) anatase and (b) rutile. Depending of the phase structure of TiO_2, it can be employed for diverging applications. The TiO_2 in anatase phase could accomplish the degradation of organic pollutants and be used in photovoltaic devices [7, 8]. The rutile TiO_2, being a bio- compatible material for blood, can be used as artificial heart valves [9]. The fabrication of nanostructured TiO_2 thin films has been achieved by several methods such as sol–gel, dip and spin coating, chemical vapor deposition (CVD), sputtering, pulsed laser deposition etc. [10–12]. In the case of sol–gel and dip coating, controlling the morphology and thickness of the film is one of the biggest challenges un- til now [13, 14]. Other methods such as physical vapor de- position (PVD) and CVD are capable of producing highly transparent films but they are expensive and also need high- vacuum systems [15].

The development of new cost-effective techniques and methods for fabrication of thin-film devices with high purity and large-area transparent films has attracted many re- searchers recently. With this motivation, we employed the electrohydrodynamic atomization (EHDA) technique for the fabrication of nanostructured TiO_2 thin films. EHDA is one of the innovative techniques to produce thin films at a high deposition rate and moreover it is cost effective [16]. EHDA works on the principle of applying electrical and mechanical energy to a liquid jet containing the precursor and allowing that to disintegrate into small nanosized droplets which de- posit on a substrate [17, 18].

The electrospray deposition of TiO_2 thin films has been reported in the literature by Mahalingam and Edirisinghe [19] and the present study can be called an improvement of the study carried out by Mahalingam and Edirisinghe. In their study, a higher voltage, 4.5 kV, was utilized for the electrospray deposition while in the present study the electrospray deposition has been carried out at almost half of the voltage requirements. Also, their Field Emission Scanning Electron Microscope (FE-SEM) analysis revealed that the morphology of as-deposited films was homogeneous and particle size was ∼1 μm, while in this paper the morphology of as-deposited TiO_2 thin films has been reported where particle size of <80 nm was achieved by using polyvinylpyrrolidone (PVP) as a stabilizer and 40 5 nm was achieved at an annealing temperature of 450°C with very good film morphology. Furthermore, a comparable transmittance in the visible region has been achieved at 450°C. Some more characterizations are discussed in this study where Fourier transform infrared (FTIR) spectroscopy and X-ray photoelectron spectroscopy (XPS) analyses of the deposited films have been carried out to complete the functional group and chemical and electronic states of the TiO_2 and electrical characterization has been done to check the applicability of electro hydrodynamically deposited TiO_2 films as functional material in optoelectronic and microelectronic applications.

Exp. Theo. NANOTECHNOLOGY 3 (2019) 103-114

2. MATERIALS AND METHODS

2.1 Preparation of precursor solution

Titanium (IV) isopropoxide (Ti*(*OCH*(*CH_3*)*$_2$*)*$_4$) and poly- vinylpyrrolidone (PVP) were purchased from Sigma-Aldrich and ethanol from Dang Chemicals. All chemicals were used in this experiment without further purification. The prepa- ration of precursor solution for the fabrication of TiO_2 thin films using EHDA is given as follows: 0.4 g of PVP was dissolved in 25 ml of ethanol solution and vigorously stirred for 15 min at 500 rpm. Then, 4 ml of titanium (IV) isopropoxide was introduced into that solution and stirring was continued for 1 h at 1000 rpm. Finally, a stable solution of precursor sol was achieved and used for further experiments and characterization.

a. Working of EHDA

The block diagram of the EHDA is represented in Fig. 1a and a photograph of the EHDA setup used in the experiment is shown in Fig. 1b. The precursor solution for the prepara- tion of TiO_2 was filled in the syringe (Hamilton, model 1001 GASTIGHT syringe), which was driven by a syringe pump (Harvard Apparatus, PHD 2000 Infusion). The syringe was connected to the capillary nozzle holder via a Teflon tube. A stainless-steel nozzle (NanoNC) with an internal diameter of 430 µm and an external diameter of 610 µm was fixed at the bottom of a nozzle holder. A high potential was ap- plied between the nozzle and the copper plate (ground) using a high-voltage DC power source (NanoNC, 30 kV) and the substrate (glass) was mounted on the copper plate. The movement of the substrate and nozzle holder could be con- trolled via the x-, z-axis stage and the y-axis stage, respectively. The whole experimental process was monitored by using a CCD camera (MotionPro X) which was interfaced with a high-performance PC.

Exp. Theo. NANOTECHNOLOGY 3 (2019) 103-114

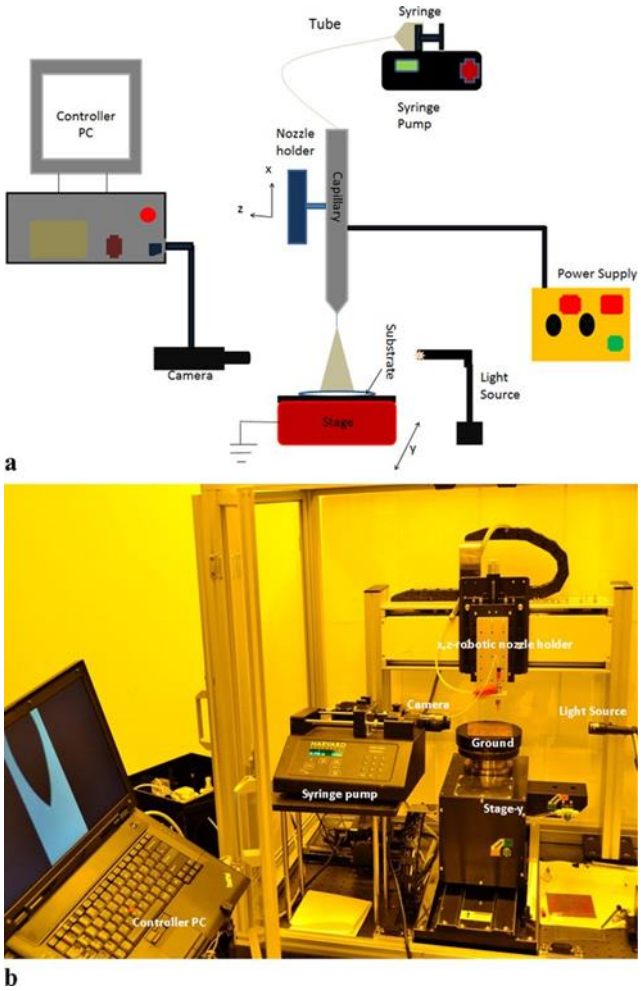

Figure 1 (a) Electrohydrodynamic atomization (EHDA) block diagram. (b) Electrohydrodynamic atomization setup

b. Preparation of TiO_2thin films using EHDA

The TiO_2 thin film was prepared on a Corning glass 7059 substrate through EHDA at room conditions with a substrate speed of 0.30 mm/s. The distance between the capillary and the substrate (standoff distance) was 6 mm. Before the de- position process, the glass substrate was sonicated with ace- tone and ethanol, rinsed with deionized water and then ir- radiated under UV light in a UV cleaner for 20 min and subjected to plasma treatment to convert the nature of the surface of the glass to be hydrophilic. The deposited films were annealed at 450°C for 2 h before the characterization process.

c. Characterization techniques

The electrical conductivity of the precursor solution was measured by a conductivity meter (EUTECH Instruments, ECOSCAN CON 6). The surface tension of the precursor sol was measured by a surface tension meter (SEO-Phoenix). The viscosity of the sol was measured

by a viscometer (ARES, TA Instruments, USA). The crystallinity and phase purity of the prepared TiO_2 thin films were analyzed us- ing an X-ray diffractometer (Rikagu D/MAX 2200H, Bede model 200).

3. RESULTS AND DISCUSSION

3.1 Characterization of precursor sol

In this work, the precursor sol was prepared using titanium isopropoxide in ethanol with PVP as a stabilizer. The addition of PVP is to improve the uniformity of the deposited thin films. The physical properties of the precursor were an important predetermining factor for the atomization process. The surface tension, electrical conductivity and viscosity of the precursor were measured as 28 mN/m, 4.9 µS/cm and
1.40 mPa s, respectively.

3.2 Taylor cone and spray formation

The EHDA experiment usually starts from a minimum flow rate and continues to a maximum flow rate (50 to 450 µl/h in this case) with various voltages in order to obtain different atomization modes such as dripping, microdripping, pulsating cone jet, stable cone jet and multi-jet. This process is used to optimize the flow rate and applied voltage for the stable cone-jet mode of spray. The possible operating envelope is shown in Fig. 2a. Figure 2b shows the different modes of atomization captured by a high-speed CCD cam- era with a constant flow rate of 200 µl/h at different voltages. The dripping and microdripping modes appeared from zero voltage until to 2.1 kV, while the spindle mode started appearing at 2.1 kV. The pulsating cone jet appeared at 2.5 kV. The stable cone jet formed at 2.7 kV and it remained until the multi-jet formed at 3.2 kV. Increasing the applied voltage after 3.2 kV led to jet discharge. A flow rate of 200 µl/h was used throughout the experiment. If the flow rate had been too small, the cone jet would not have remained stable for a long period of time.

According to the classical electrohydrodynamic atomization of the stable cone jet mode, the electrical relaxation time, T_e, must be very much smaller than the hydrodynamic time, T_h [20]. It is established by the inequality diffraction intensity was recorded in the 2θ range 20– 70° with a step of 0.02°. The TiO_2 film was investigated by a FTIR analyzer (Bruker IFS 66/S, Germany) for analysis of functional groups present in the film. The surface morphology and the structure of deposited films were investigated by a field emission scanning electron microscope (JEOL, JEM 1200EX II). X-ray photoelectron spectroscopy (XPS) measurements were carried out using an ESCA 2000 VG Microtech system. The transparency of the films was recorded by a UV/vis/NIR spectrometer (Shimadzu UV-3150) with a range of 200–700 nm. The I –V characteristics of the TiO_2 thin films were measured by a semiconductor device (B1500A, Agilent, USA) parameter analyzer.

Exp. Theo. NANOTECHNOLOGY 3 (2019) 103-114

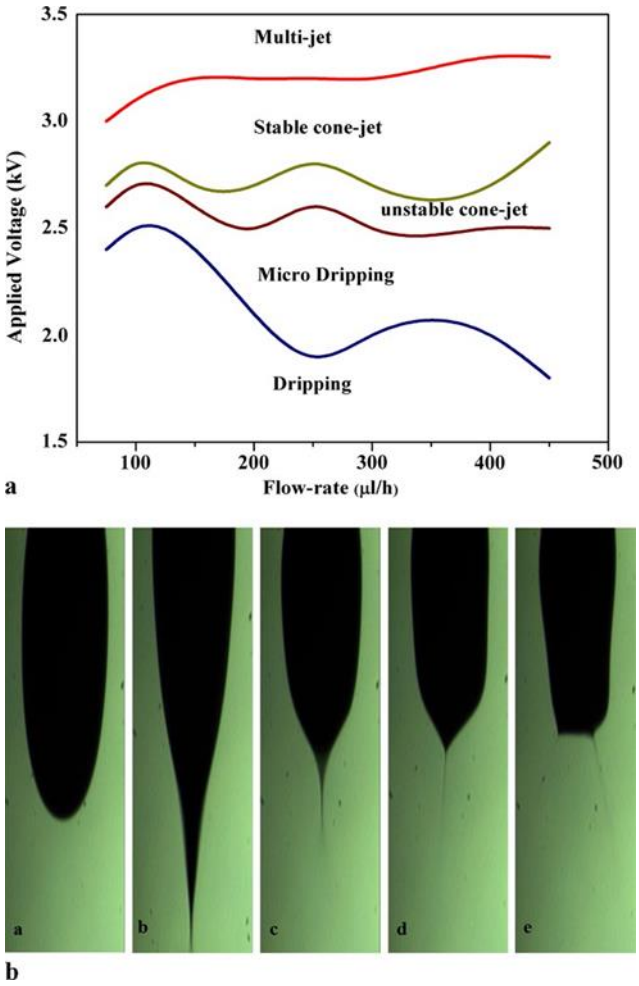

Fig. 2 (a) Operating envelope of precursor sol. (b) Modes of atomization.

3.3 XRD analysis of TiO_2 thin films

The XRD patterns of TiO_2 thin films annealed at 450°C are presented in Fig. 3. The presence of peaks revealed the formation of nanocrystalline TiO_2 film. It showed Bragg reflection at 2θ values of 25.4°, 37.6°, 48°, 53.6°, 54.9°, 62.7°, 68.6°, 69.8°and 75°, indicating the characteristic peak of tetragonal crystal planes of anatase phase TiO_2 [21], suggesting the high quality of the TiO_2 thin films. No peak corresponding to the rutile phase of TiO_2 was seen in the diffractogram, suggesting clearly that only anatase phase has been formed. Moreover, the average crystallite size was estimated by using the Debye–Scherrer (DS) equation [22].

3.4 Surface morphology using scanning electron microscope

The surface morphology of the TiO_2 thin films was mea- sured by using scanning electron microscopy (SEM). As shown in Fig. 4a and b, the SEM image reveals that the as- deposited TiO_2 thin film was very homogeneous with much less agglomeration of particles due to using PVP, which leads to the prevention of the particle agglomeration. Fig- ure 4c and d show the uniform morphology of the annealed TiO_2 thin film. The grain size was measured as 40 5 nm with spherical morphology as shown. The grain size from the SEM studies is in accord

±

with the XRD results shown in the previous subsection. At 450°C deposited particle rearrangement takes place and the film becomes well crystalline in nature. The main advantage of EHDA lies in the fact that the deposition pro- cess is very simple and is carried out at room temperature. Accomplishment of the presented results at room conditions and open environment is an achievement.

3.5 FTIR analysis

The FTIR spectra of TiO_2 thin films (as-deposited and annealed at 450°C) are shown in Fig. 5a and b. The spectra of the as-deposited film shows the presence of Ti–O stretching around 500 to 800 cm^{-1} [23]. It also shows the peaks cor- responding to the organic components present in the PVP stabilizer in the region 1000 cm^{-1} to 1400 cm^{-1} corresponding to the pyridine ring (C_4H_8N–) in the PVP [24]. It also exhibited the peak corresponding to hydroxyl groups (O–H stretching) or water content in the region 1620 and 3500 cm^{-1} [25]. After annealing the thin film at 450°C for h, the Ti–O peak becomes narrowed in the region 450 to 600 cm^{-1} which is due to the transformation of $Ti(OH)_2$ into TiO_2 [26]. Here the presence of organic residues due to the stabilizer PVP in the as-deposited film is removed completely in the spectra of the films annealed at 450 °C.

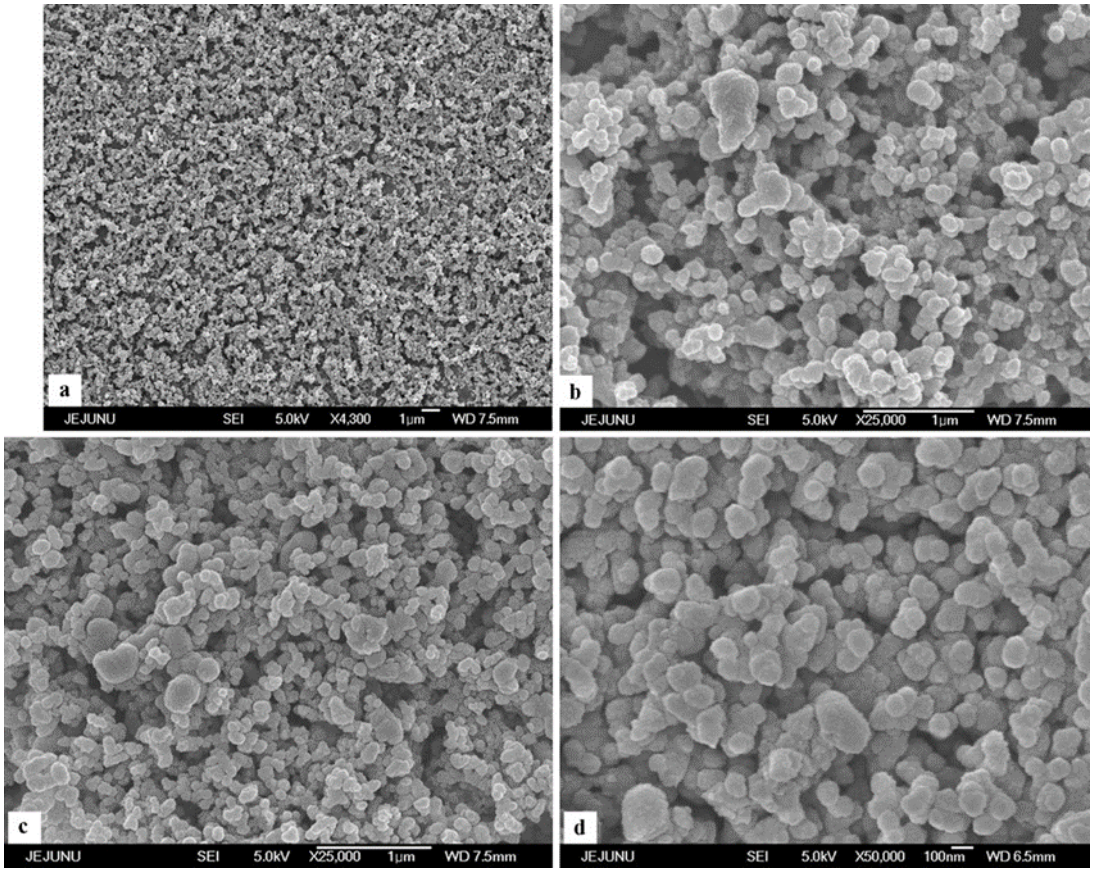

Figure 4 SEM observation of TiO2 thin films: (a), (b) as-deposited and (c), (d) annealed at 450 °C.

Exp. Theo. NANOTECHNOLOGY 3 (2019) 103-114

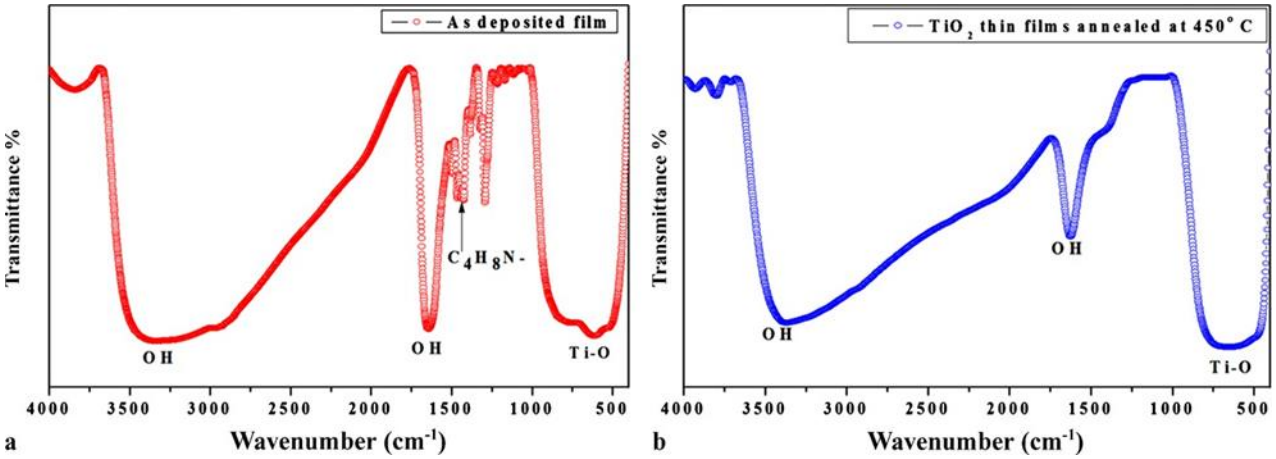

Figure 5 FTIR spectra of TiO2 thin films: (a) as-deposited and (b) annealed at 450 °C.

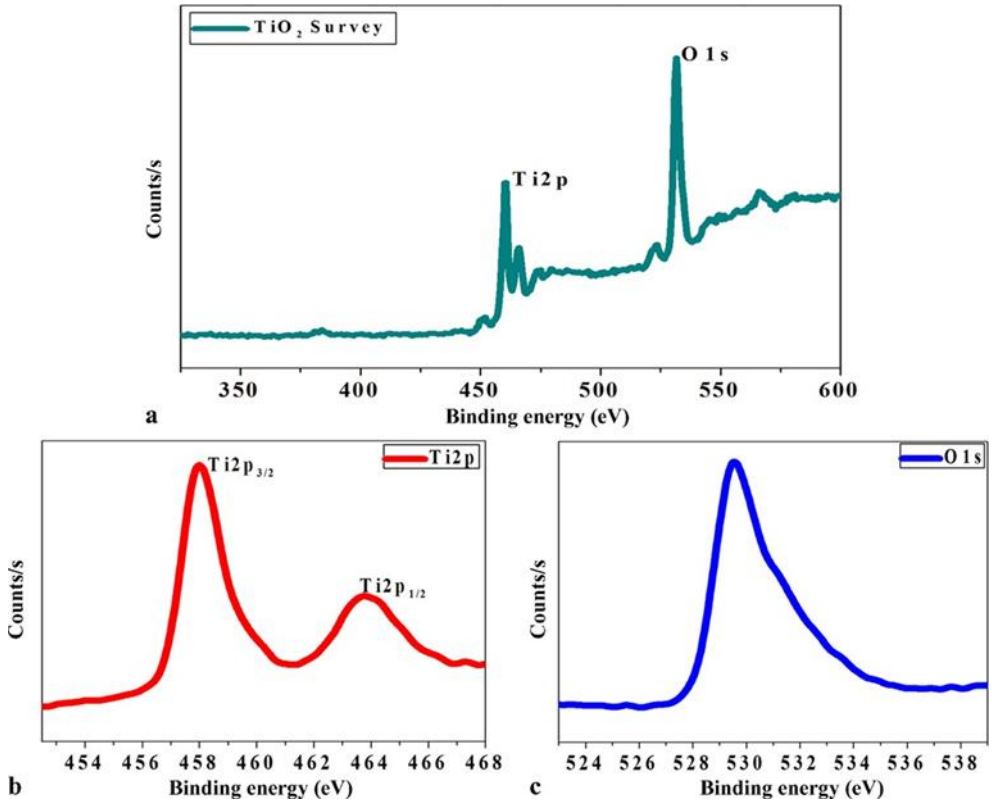

Figure 6 XPS spectra of TiO2 thin films deposited using EHDA.

3.6 X-ray photoelectron spectroscopy (XPS) analysis

The X-ray photoelectron spectrum of the TiO_2 thin films deposited by the EHDA technique is shown in Fig. 6a showing the presence of Ti2p and O1s [27]. The decon- voluted spectrum of Ti2p (as shown in Fig. 6b) exhibited the characteristic peaks of $Ti2p_{3/2}$ and $Ti2p_{1/2}$ with the cor- responding binding energies $E_b(Ti2p_{1/2})$ = 464.05 eV and $E_b(Ti2p_{3/2})$ 458.4 eV, respectively. In the case of oxygen, the high-resolution spectrum of O1s had a peak in 529.5

eV that corresponds to the TiO_2 binding energy, as shown in Fig. 6c. No characteristic peaks of any impurities were detected in the XPS analysis, suggesting that high-quality TiO_2 thin films were obtained.

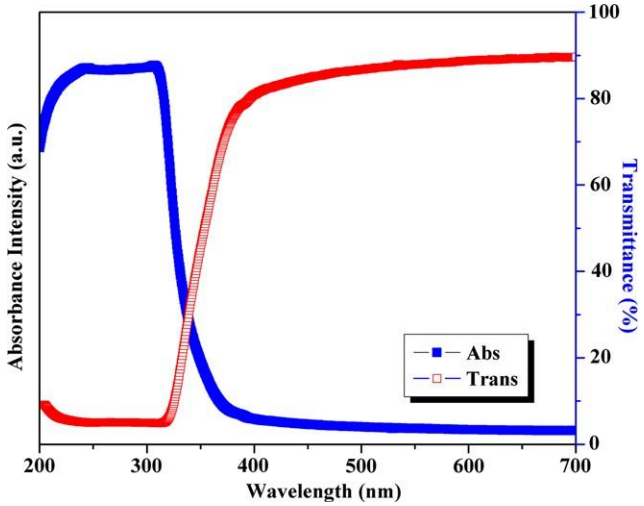

Fig. 7 UV-vis spectra of TiO2 thin films showing the absorbance and transmittance curves

3.7 Optical properties

The optical properties of the TiO2 thin films annealed at 450°C were characterized by UV-vis spectroscopy as shown in Fig. 7. The transmittance spectrum of the TiO2 film showed that it has 85% transmittance in the visible region. The op- tical band gap energy from the UV-vis spectra can be esti- mated by using the following equation [28].

The band gap was estimated from a plot of (αhν)1/2 versus photon energy (αhν). The intercept of the tangent to the plot gave a good approximation to the band gap energy for this indirect band gap material. Figure 8 shows the optical band gap calculation scheme of the deposited film: it was found as 3.45 eV and the absorption edge was red shifted.

The aver- age value of the band gap of the bulk anatase is 3.2 eV [29]. The band gap widening in the TiO2 films is mainly attributed to the contribution of crystallite size effects [30, 31].

3.8 Electrical characterization

Figure 9 shows the current–voltage (I –V) measurement characteristic of TiO2 thin films. The electrodes were made by silver (Ag) using silver ink (NPK Ink Ltd.) deposited by the EHDA method [32].

4. CONCLUSIONS

In conclusion, nanostructured TiO_2 thin films on glass substrates were prepared using the EHDA technique. The process parameters of the EHDA spray for the achievement of uniform films were discussed. The XRD results indicated that TiO2 films were oriented in the anatase phase. SEM studies revealed the uniform morphology of TiO_2 thin films due to the influence of PVP as a stabilizer. The FTIR and XPS results confirmed that the TiO2 was present in the

films without any organic residue, suggesting the high pu- rity of the method. The EHDA-deposited TiO_2 films exhibited more than 85% transparency and the optical band gap of the TiO_2 films was found to be 3.45 eV. The band gap widening in the TiO_2 films is mainly attributed to the contribution of crystallite size effects. The I –V characteristic of the deposited films shows good ohmic behavior with a sheet resistance of 45 mQ cm. Our key findings in this work can provide new positive features in the utilization of EHDA techniques for future device applications.

References

[1] C. Monat, B. Alloing, C. Zinoni, L.H. Li, A. Fiore, Nano Lett. 6, (2006) 1464
[2] M. Krunks, A. Katerski, T. Dedova, I. Oja Acik, A. Mere, Sol. Energy Mater. Sol. Cells 92, (2008) 1016
[3] K. Narashimha Rao, S. Mohan, J. Vac. Sci. Technol., A, Vac. Surf. Films 8, (1990) 3260
[4] M.R. Hofmann, S.T. Martin, W. Choi, D.W. Bahnemann, Chem. Rev. 95, (1995) 69
[5] T. Fuyuki, H. Matsunami, Jpn. J. Appl. Phys. 25, (1986) 1288
[6] A.L. Linsebigler, G. Lu, J.T. Yates, Chem. Rev. 95, (1995) 735
[7] C.-K. Jung, S.B. Lee, J.-H. Boo, S.-J. Ku, K.-S. Yu, J.-W. Lee, Surf. Coat. Technol. 174–175, (2003) 296
[8] S. Takeda, S. Suzuki, H. Odaka, Thin Solid Films 392, (2001) 338
[9] F. Zhang, N. Huang, P. Yang, Surf. Coat. Technol. 84, (1996) 476
[10] D.J. Kim, J.O. Baeg, S.J. Moon, K.S. Kim, J. Nanosci. Nanotechnol. 9, (2009) 4285
[11] N. Voudouris, G.N. Angelopoulos, Surf. Coat. Technol. 115, (1999) 38
[12] C. Vahlas, B. Caussat, P. Serp, G.N. Angelopoulos, Mater. Sci. Eng., R Rep. 53, (2006) 1
[13] K.S. Kim, D.J. Kim, J. Aerosol Sci. 37, (2006) 1532
[14] A. Jaworek, A. Krupa, J. Aerosol Sci. 30, (1999) 873
[15] A.M. Ganan-Calvo, J. Davila, A. Barrero, J. Aerosol Sci. 28, (1997) 249
[16] C.J. Luo, S. Loh, E. Stride, M. Edirisinghe, Food Bioprocess. Technol. (2011). doi:10.1007/s11947-011-0534-6
[17] S.N. Jayasinghe, M.J. Edirisinghe, J. Aerosol Sci. 33, (2002) 1379
[18] S.N. Jayasinghe, M.J. Edirisinghe, J. Mater. Sci. Lett. 37, (2002) 1987
[19] S. Mahalingam, M.J. Edirisinghe, Appl. Phys. A 89, (2007) 987
[20] A.M. Ganan-Calvo, J. Davila, A. Barrero, J. Aerosol Sci. 28, (1997) 249
[21] D. Wang, C. Song, Y. Lin, Z. Hu, Mater. Lett. 60, (2006) 77
[22] K. Karthikeyan, N. Poornaprakash, N. Selvakumar, K. Jeyasubrmanian, J. Nanostruct. Polym. Nanocompos. 5, (2009) 83
[23] J. Zhang, I. Boyd, B.J. O'Sullivan, P.K. Hurley, P.V. Kelly, J.-P. Senateur, J. Non-Cryst. Solids 303, (2002) 134
[24] P.K. Khanna, R. Gokhale, V.V.V.S. Subbarao, J. Mater. Sci. 39, (2004) 5956
[25] R. Zhang, L. Gao, Key Eng. Mater. 224–226, (2002) 573
[26] Y. Zhu, T. Liu, C. Ding, J. Mater. Res. 14(2), (1999) 444
[27] W. Zhang, S. Zhu, Y. Li, F. Wang, J. Mater. Sci. Technol. 20, (2004) 31
[28] K. Krishnamoorthy, R. Mohan, S.-J. Kim, Appl. Phys. Lett. 98, (2011) 244101
[29] Y. Lei, L.D. Zhang, J.C. Fan, Chem. Phys. Lett. 338, (2001) 231
[30] K. Mogyorosi, I. Dekany, J.H. Fendler, Langmuir 19, (2003) 2938
[31] G. Lei, X. Mingxia, F. Haibo, S. Ming, Appl. Surf. Sci. 253, (2006) 720
[32] A. Khan, K. Rahman, M.-T. Hyun, D.-S. Kim, K.H. Choi, Appl. Phys. A 104, (2011) 1113
[33] A. Bearzotti, A. Bianco, G. Montesperelli, E. Traversa, Sens. Actuators Chem. B 19, (1994) 525
[34] A. Orendorz, J. Wusten, C. Ziegler, H. Gnaser, Appl. Surf. Sci. 252, (2005) 85

[35] W.G. Kim, S.W. Rhee, Microelectron. Eng. 86, (2009) 2153
[36] M. Mourad Mabrook, Exp. Theo. NANOTECHNOLOGY 2 (2018) 103

Exp. Theo. NANOTECHNOLOGY 3 (2019) 103-114